JOURNAL OF Materials Feature Article CHEMISTRY

Molecular design of hybrid organic–inorganic nanocomposites synthesized *via* sol–gel chemistry†

C. Sanchez, F. Ribot and B. Lebeau

Chimie de la Matière Condensée, UMR CNRS 7574, Université Pierre et Marie Curie 4, place Jussieu, 75252 Paris, France. E-mail: clems@ccr.jussieu.fr

Received 12th May 1998, Accepted 16th July 1998

The design, synthesis and some optical properties of hybrid organic–inorganic nanocomposites materials are presented. The properties that can be expected for such materials depend on the chemical nature of their components, but they also depend on the synergy of these components. Thus, the interface in these nanocomposites is of paramount significance and one key point of their synthesis is the control of this interface. These nanocomposites can be obtained by hydrolysis and condensation reactions of organically functionalized alkoxide precursors. Striking examples of hybrids made from modified silicon, tin and transition metal alkoxides are presented. Some optical properties (photochromic, luminescence, NLO) of siloxane based hybrids are also discussed.

1 Introduction

Sol–gel chemistry is based on the polymerization of molecular precursors such as metal alkoxides $M(OR)_n$.[1,2] Hydrolysis and condensation of these alkoxides lead to the formation of metal oxo-polymers. The mild characteristics offered by the sol–gel process allow the introduction of organic molecules inside an inorganic network.[3] Inorganic and organic components can then be mixed at the nanometric scale, in virtually any ratio leading to so-called hybrid organic–inorganic nanocomposites.[4] These hybrids are extremely versatile in their composition, processing and optical and mechanical properties.[5] The nature of the interface between the organic and inorganic components has been used recently to classify these hybrids into two different classes.[4h] Class I corresponds to all the systems where there are no covalent or iono-covalent bonds between the organic and inorganic components. In such materials, the various components only exchange interactions such as van der Waals forces, hydrogen bondings or electrostatic forces. In contrast, in class II materials, some of the organic and inorganic components are linked through strong chemical bonds (covalent or iono-covalent). Numerous hybrid organic–inorganic materials have been developed in the past few years. This development yields many interesting new materials, with mechanical properties tunable between those of glasses and those of polymers, with improved optical properties (efficiency, stability, new sensors, *etc.*) and with improved catalytic or membrane based properties.[4g] This field of materials research mainly arises from chemists' skills and demonstrates the major role played by chemistry in advanced materials.

Siloxane based hybrids[4] can be easily synthesized because $Si-C_{sp^3}$ bonds are rather covalent and therefore they are not broken upon hydrolysis. Similar chemistry can be developed from tin alkoxides. This is not aplicable to transition metals for which the more ionic M—C bond is easily cleaved by water; complexing organic ligands must be used. Such groups can be functionalized for any kind of organic reactions such as organic polymerization and lead to hybrid organic–inorganic copolymers.[6–8] This article reviews some of the previous work we have performed on the design and synthesis of hybrid organic–inorganic nanocomposites in which organics are simply embedded or chemically bonded to the inorganic gel network.

2 Siloxane based hybrid materials

Organic groups can be bonded to an inorganic network as network modifiers or network formers. Both functions have been achieved in the so-called ORMOSILS.[3,9] The precursors of these compounds are organo-substituted silicic acid esters of general formula $R'_nSi(OR)_{4-n}$, where R′ can be any organofunctional group. If R′ is a simple non hydrolyzable group bonded to silicon through a Si—C bond, it will have a network modifying effect ($Si-CH_3$). On the other hand, if R′ can react with itself (R′ contains a methacryl group for example) or additional components, it will act as a network former.[3c] Network modifiers and network formers can also introduce other physical properties (mechanical, hydrophobic, electrochemical, optical, *etc.*). Several examples related to some optical properties of siloxane based hybrids will be now described.

2-A Photochromic properties

Spiropyrans and spirooxazines are two of the fascinating families of molecules exhibiting photochromic properties. Upon irradiation, the colorless spiropyran or spirooxazine undergoes heterolytic C—O ring cleavage, producing colored forms of merocyanines (Fig. 1).

The merocyanines may interact with their environment, *i.e.* solvent, matrix, *etc.* leading to different photochromic responses. Levy and Avnir[10] first demonstrated the important role played by the dye–matrix interactions on the photochromic response of spiropyrans. They studied the photochromism of spiropyrans trapped in sol–gel matrices synthesized *via* polymerization of $Si(OCH_3)_4$ or $RSi(OEt)_3$ (R = ethyl,

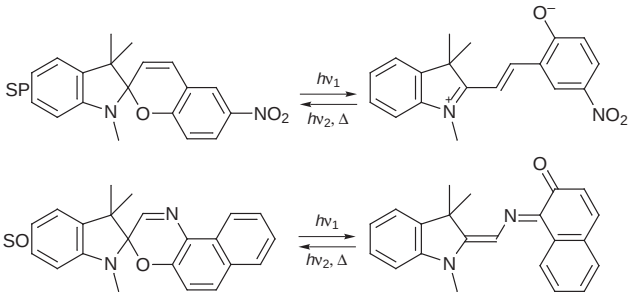

Fig. 1 Molecular structures of SO and SP photochromic dyes.

†Basis of the presentation given at Materials Chemistry Discussion No. 1, 24–26 September 1998, University of Bordeaux, France.

methyl, *etc.*) precursors, and observed two types of photochromic behavior.

When the photochromic dye is trapped within a hydrophilic domain of the matrix (domain containing residual Si—OH groups), the open zwitterionic colored forms are probably stabilized through hydrogen bonding with the acidic silanol groups present at the pore surface. The result of this stabilization is the observation of the colored forms before irradiation. These colored forms can be bleached by irradiation in the visible range. This has been termed 'reverse photochromism'. On the other hand spiropyran dyes embedded in a more hydrophobic hybrid network made by hydrolysis of $RSi(OEt)_3$ exhibit direct photochromism, *i.e.* the colorless form is stable without irradiation. Such photochromic behavior has been reported for many spiropyran or spirooxazine doped sol–gel matrices.[10–17] Moreover, for hybrid organic–inorganic matrices containing different chemical environments (hydrophilic and hydrophobic domains) a competition between direct and reverse photochromisms can be observed.[17] However many fundamental questions still need to be considered. Little is known concerning the role of the photochromic dye–matrix interactions in the kinetics of coloration and thermal fading. As far as photochromic devices are concerned the tuning between strong and fast photochromic coloration (high ΔA) and very fast thermal fading is needed. Usually spiropyran or spirooxazine doped sol–gel matrices or even spirooxazine doped polymeric matrices exhibit slow thermal fading.[10–18]

The photochromic behavior of a spiropyran SP (6-nitro-1′,3′,3′-trimethylspiro{2*H*-1-benzopyran-2,2′-indoline}) and a spirooxazine SO (1,3,3-trimethylspiro{indoline-2,3′(3H)-naph(2,1-*b*)(1,4)oxazine}) (Fig. 1) embedded within two new hybrid matrices have been recently studied.[19]

Photochromic properties of the SP or SO doped D/Zr hybrid matrices. The first kind of matrix obtained through hydrolysis and condensation of $(CH_3)_2Si(OC_2H_5)_2$ (D) and appropriate amounts of $Zr(OPr^n)_4$ (Zr) is labelled D/Zr*x*, where Zr stands for the zirconium, *x* for the molar amount of zirconium.

These D/Zr*x* matrices are hybrid nanocomposites made from polydimethylsiloxane species (chains, cycles *etc.*) crosslinked by zirconium oxopolymers.[20–22] The zirconium oxopolymers are hydrophilic domains that still contain some hydroxo groups coming from residual ethanol or Zr—OH ligands.[22] The size and the spacing between the ZrO_2 based domains is about a few nanometers as evidenced by SAXS.[22] ^{17}O MAS NMR and FTIR experiments show that inside these composites the hydrophobic polydimethylsiloxane species are interfaced with the zirconium oxo domains both through covalent Zr—O—Si bonds and through weak interactions (hydrogen and van der Waals bonds).[19] The structure of the D/Zr*x* matrices is shown schematically in Fig. 2. D/Zr*x* matrices doped with SP or SO are lightly colored (pink with SP or blue with SO) before irradiation. However the absorbance (A) in the visible region is weak in comparison with the total amount of embedded photochromic dyes. The amount of colored form depends on the *x* content.

Fig. 3 shows the photochromic behavior of SP doped D/Zr*x* gels for three compositions of zirconium. When the Zr amount increases, the A variation due to the coloration decreases while that due to the decoloration increases: there are more and more open forms in the gel. The amount of colored form increases proportionally with the *x* content. It is much higher for D/Zr30 samples than for D/Zr10 ones.

This indicates that before irradiation the SO and SP dyes are roughly split into two populations. The colored merocyanine open forms of SO and SP are stabilized by hydrogen bonding within the hydrophilic regions made from the zirconium oxopolymers, while the closed SO and SP forms are probably located in the environment of the hydrophobic polydimethylsiloxane chains. So for these D/Zr*x* matrices the photochromism is partially reversed and can be balanced by tuning the D/Zr ratio.

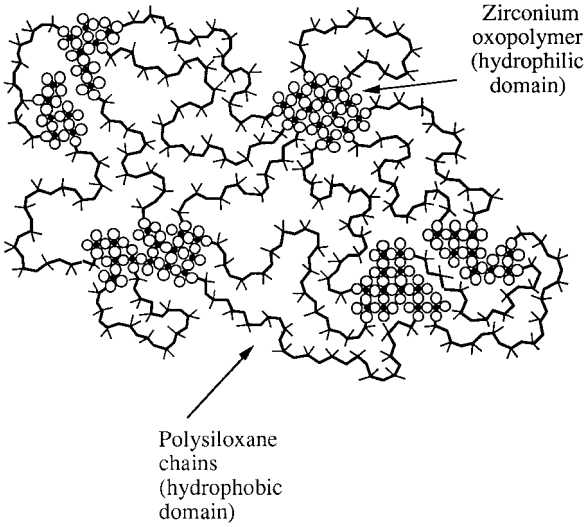

Fig. 2 Cartoon of the D/Zr*x* matrices.

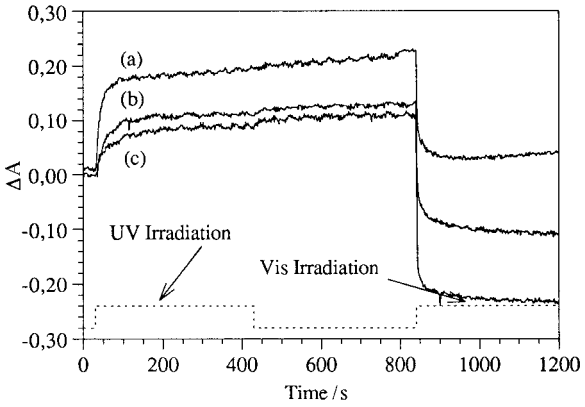

Fig. 3 Photocolouration and photobleaching of SP doped D/Zr*x* matrices[19] [(a) $x=10$; (b) $x=20$; (c) $x=30$].

The thermal bleaching behavior of the D/Zr20 samples was fitted with a biexponential equation. The SP doped materials exhibited a very long bleaching time (about 24 h) while for the SO doped D/Zr20 materials the thermal fading was much faster.[19]

The kinetic data of the SP or SO doped D/Zr20 samples are similar to those reported for other modified sol–gel matrices or in organic polymers.[17,23] As in organic polymers, the bleaching follows a biexponential equation which can be explained by an inhomogeneous distribution of free volumes in the gel. Moreover the presence of different stereoisomers (*cis* or *trans*) could also account for this behavior. The different isomer–matrix interactions could explain the different kinetics observed for SO and SP.

The thermal fading is longer for SP doped hybrids than for SO doped ones. This phenomenon can be correlated to the fact that SP open forms are known for their tendancy to form zwitterionic species, while non charged quinonic species are usually favored for open SO molecules. Zwitterionic species can be strongly stabilized by hydrogen bonding with the matrix, thus lowering the decay times of thermal fading.

Photochromic properties of the SP or SO doped DH/TH hybrid matrices. The second kind of SP or SO doped matrix prepared from the hydrolysis and cocondensation of $(CH_3)HSi(OC_2H_5)_2$ (DH) and $HSi(OC_2H_5)_3$ (TH) precursors is labelled DH70/TH30 (70/30 refers to the molar composi-

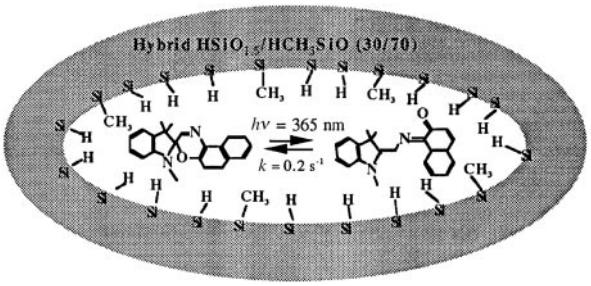

Fig. 4 Schematic representation of the environment experienced by the SO dye within the matrix DH70/TH30.

tion). These hybrids can be described as strongly interpenetrated nanocomposites. The environment experienced by the SO dye within the DH70/TH30 matrix is shown in Fig. 4.

The SO or SP DH70/TH30 doped matrices exhibit normal photochromism. All the samples are colorless before irradiation. For the two photochromic dyes, the thermal fading can be fitted with excellent agreement with a monoexponential equation. This may be related to the quasi-liquid mobility observed by NMR for this matrix.

The time dependence of the absorption upon repeated irradiation with 365 nm light for SO doped DH70/TH30 coatings is reported in Fig. 5. The photochromic behavior is reversible, extremely fast (the rate constant is 0.2 s^{-1}) and corresponds to a very high absorption jump ($\Delta A = 1.2$). The photochromic kinetics of these SO doped hybrid materials are to the best of our knowledge much faster than those reported for SO in any other matrix (sol–gel matrices, organic polymers, alcohols, *etc.*).[11,14,15,17,23]

The very high reactivity of the DH/TH precursors towards hydrolysis–condensation reactions (Si—OH groups are immediatly consumed) and the strong hydrophobicity of the resulting matrix are both responsible for the direct and very fast photochromic behavior observed.

2-B Luminescent properties of rare-earth doped hybrids

Neodymium doped sol–gel matrices are suitable luminescent materials. However room temperature sol–gel derived matrices usually contain a large amount of hydroxy groups which are responsible for the quenching of the Nd^{3+} emission. Therefore the design of sol–gel matrices inside which the hydroxy content can be minimized[24,25] and/or inside which the rare earth is protected *via* complexation[26] or encapsulation is desirable. Recent work has demonstrated fluorescence emission for the Nd^{3+}, Sm^{3+}, Dy^{3+}, Er^{3+} and Tm^{3+} ions doped in hybrid siloxane–oxide matrices.[25]

These hybrids were synthesized by the following procedure. Diethoxymethylsilane [DEMS = $SiH(OEt)_2(CH_3)$], absolute ethanol and water in a 1 : 1 : 1 molar ratio were mixed for a few minutes under magnetic stirring. A solution of mixed alkoxides, $Zr(OPr^n)_4$ and a corresponding rare earth (M = Nd^{3+}, Sm^{3+}, Dy^{3+}, *etc.*) methoxy ethoxide was then added to the previous solution in order to obtain a Zr : Si molar ratio of 1 : 9 and M : Si molar ratios of 1 : 9; 0.1 : 9; 0.01 : 9. The sols were deposited onto glass sheets and allowed to gel and dry at room temperature. Such transparent coatings were deposited several times till a thin layer of about 50–100 μm was obtained.[25]

FTIR, ^1H MAS NMR and ^{29}Si CP MAS NMR experiments have shown that these hybrids can be described as nanocomposites built from siloxane polymers crosslinked by metal oxo species. The metal oxo domains are made of mixed zirconium–rare earth oxo species.

Absorption–emission properties of these Nd^{3+} doped hybrid coatings. The room temperature absorption spectrum of Nd^{3+} doped hybrid coatings presented in ref. 25 consisted of some broad transitions. The $^4I_{9/2} \rightarrow {}^4F_{5/2}, {}^2H_{9/2}$ transition around 800 nm, particularly important for diode pumping systems, presents a FWHM of around 15 nm. The absorption coefficient at this wavelength is around 10 cm^{-1} for a coating containing approximately 4×10^{20} Nd^{3+} ions cm^{-3}. This high absorption coefficient value indicates that a high Nd^{3+} concentration could be introduced into the system without affecting the synthesis and the transparency of the films.

For Nd^{3+} ions excited at 805 nm, the emission spectra of the $^4F_{3/2} \rightarrow {}^4I_{11/2}$ transition at room temperature is presented in Fig. 6. This emission is broad with a FWHM around 40 nm and extends into the NIR range from approximately 1.045 to 1.095 μm. A broad emission has also been observed for the $^4F_{3/2} \rightarrow {}^4I_{9/2}$ transition.[25] Broad emissions for Nd^{3+} are characteristic of wide sites distribution around the neodymium ions in this hybrid materials. Such inhomogeneous broadening is also observed in glassy hosts.[27,28] Experimentally, one can notice that the Nd^{3+} fluorescence intensity is weaker than those reported in glassy or crystalline matrices where the quantum efficiency is relatively high.[29]

Fluorescence kinetics of Nd^{3+} in hybrid siloxane based coatings. Fig. 7 presents the variation of the fluorescence intensity decay profiles as a function of the Nd^{3+} content. Lifetimes decrease from 160 μs for 0.4×10^{20} Nd^{3+} ions cm^{-3} to approximately 200 ns for 4×10^{21} Nd^{3+} ions cm^{-3}.

It is quite unusual to observe radiative emission of Nd^{3+} ions in matrices prepared at room temperature by sol–gel processing. Usually the numerous hydroxy groups present in classical xerogels obtained at room temperature prevent any Nd^{3+} radiative emission.[5d,5e,32] A thermal treatment at high temperatures is necessary to allow the Nd^{3+} emission to be observed. In all our samples fluorescence is detected, however

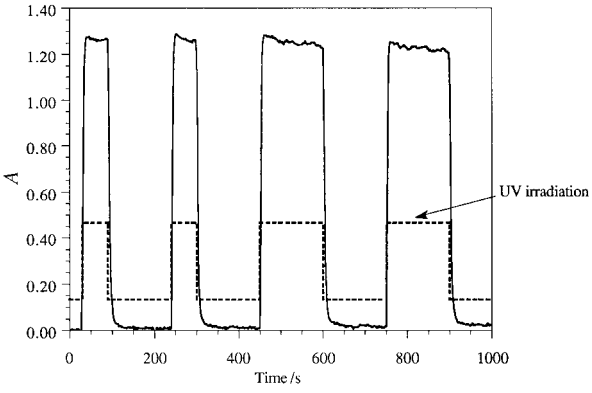

Fig. 5 Photochromic response of the SO doped DH70/TH30 matrix.[18]

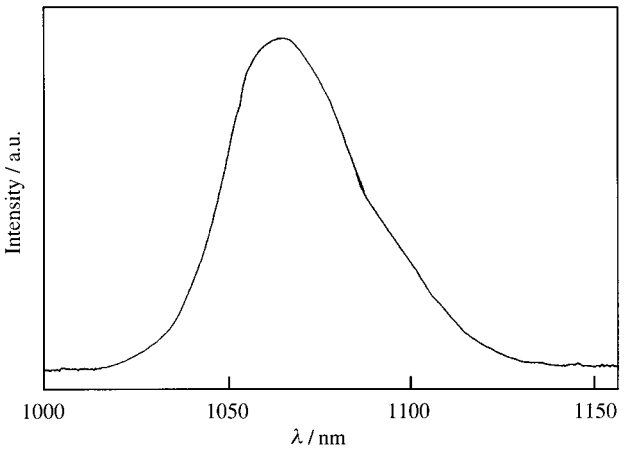

Fig. 6 RT Nd^{3+} fluorescence spectra.[30]

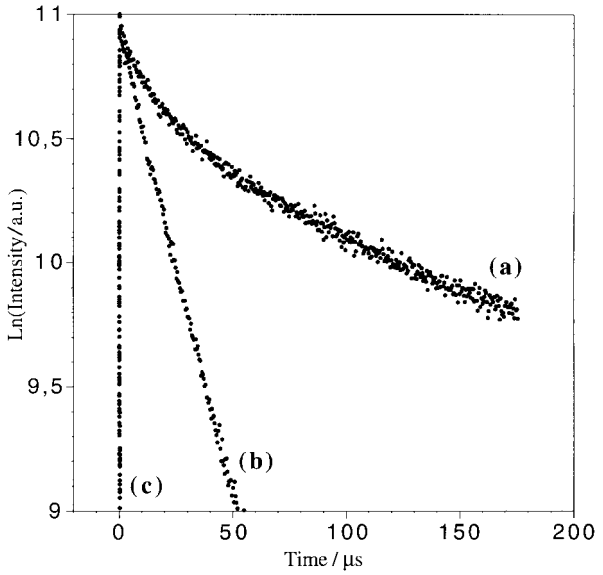

Fig. 7 Variation of the Nd^{3+} fluorescence decay[31] (Nd^{3+} content in atom cm^{-3}, (a) $0.4\times10,^{20}$ (b) 4×10^{20} (c) 4×10^{21}.

the Nd^{3+} fluorescence decay profiles lead to lifetime values lower than those usually recorded for Nd^{3+} in high temperature processed glassy or crystalline matrices. These hybrid materials can be described as a siloxane polymeric network made from ($CH_3SiO_{3/2}$) units crosslinked by mixed nanoaggregates made from zirconium oxo and neodymium oxo species.

Depending on the Nd^{3+} concentration, two different optical features are observed in these hybrid coatings. Both are well correlated with the structure. (1) For low Nd^{3+} concentration, the initial non-exponential part of the decay profiles vary linearly on a root-mean-square time scale showing the strong cross-relaxation phenomena. Even if a few ν_{O-H} vibrations are observed in the infrared spectrum, these hydroxy groups are not located close to the Nd^{3+} ions and at low concentration the main non-radiative de-excitation mechanisms are the Nd^{3+}–Nd^{3+} interactions. The fact that these nanocomposites are made with segregated metal oxo species (the dispersion is not statistical all over the sample) leads to Nd^{3+}–Nd^{3+} interactions even for low rare earth concentrations. The slope measured at long times give an indication of the Nd^{3+} fluorescence quantum yield in this hybrid coating. The ratio η of the experimental lifetime at low concentration over the calculated radiative lifetime ($\eta=0.35$) indicates that approximately 35% of the relaxation occurs radiatively at low Nd^{3+} concentration. This is a high value for a room temperature sol–gel processed material and this is in agreement with the fact that, at low concentration, Nd^{3+} ions form clusters at relatively long distances from the remaining hydroxy groups. (2) When the Nd^{3+} concentration increases, interactions increase as the Nd^{3+}–Nd^{3+} distance becomes shorter in the nanoaggregates. Simultaneously when the neodymium concentration increases (the zirconium concentration remaining constant) the probability of finding neodymium ions at the surface of the metal oxo species increases, rendering the rare earth prone to interactions with some remaining hydroxy groups located close to the surface. As a consequence, short lifetimes are observed. For a concentration of 4×10^{21} Nd^{3+} ions cm^{-3} the quantum yield is less than 0.01%. This behavior characterizes non-radiative de-excitation processes due to strong energy transfers between Nd^{3+} but also non-radiative de-excitation occurring *via* the filling of the $^4F_{3/2}$–$^4I_{15/2}$ energy gap by ν_{O-H} vibrations. Usually, according to the energy gap law, multiphonon non-radiative contributions do not exceed 50% taking into account the energy difference around 5500 cm^{-1} between the $^4F_{3/2}$ and $^4I_{15/2}$ levels. In the present case, phonons can interact with the atomic transitions of Nd^{3+} and this coupling, analogous to weak electric dipole coupling, is enhanced when hydroxy groups are close to the neodymium ions. These interactions may explain the low Nd^{3+} quantum efficiency values and the weak emission observed for high Nd^{3+} concentration. All these results need of course to be improved, however they open many possibilities in the field of room temperature processed luminescent films.

Energy transfer between an organic dye and Nd^{3+} as inorganic chromophore. Codoped rhodamine 6G–Nd^{3+} hybrid samples shows that the rhodamine emission spectra exhibit some dips at wavelengths corresponding to the Nd^{3+} absorption bands.[31] This feature indicates that radiative energy transfer occurs between the organic dye and the Nd^{3+} ions.[33–35] A photon emitted by the rhodamine molecule can be trapped by the rare-earth ions in the hybrid siloxane network.

Furthermore, when excited by an argon laser at 488 nm, a wavelength where only the organic dye molecules absorb, the codoped (R6G–Nd^{3+}) hybrid coating exhibits a Nd^{3+} emission around 1.06 μm. No emission was detected around 1.06 μm under the same experimental conditions without the presence of the organic dye inside the hybrid coating. This behavior reveals that energy transfer mechanisms may be favorable for Nd^{3+} emission.

New Eu^{2+} doped hybrid organic–inorganic nanocomposites synthesized at room temperature. The Eu^{2+} ion is particularly unique because its broad luminescence band $4f^65d^1\rightarrow4f^7$ is strongly host dependent with emission wavelengths extending from the UV to the red range of the electromagnetic spectrum.[36] Therefore, the luminescent properties of Eu^{2+}-doped solids have been intensively studied during the past three decades. These studies have led to the use of these compounds as phosphors, notably blue-emitting $Eu^{2+}:BaMgAl_{10}O_{17}$ in lamp and plasma display panels and UV-emitting $Eu^{2+}:SrB_4O_7$ for medical applications and skin tanning. Crystalline or glassy Eu^{2+} doped materials are usually processed at relatively high temperatures.[36–39] Moreover, the synthesis and the stabilization of europium in the divalent state under mild synthetic conditions is not an easy task. For the first time, we reported recently the room temperature synthesis of new Eu^{2+} doped hybrid materials together with their absorption and emission properties.[40] These hybrids are obtained though the hydrolysis and condensation of diethoxymethylsilane (MDES), methyltriethoxysilane (TREOS) and zirconium tetrapropoxide precursors in the presence of europium trichloride.

Dehydrocondensation of organic hydrosilanes with silanols is one of the common methods for the synthesis of the siloxane linkage.[41] This reaction, which occurs with the evolution of hydrogen gas, has been described as follows:[41]

$$\equiv Si-H + HO-Si\equiv \xrightarrow{\text{catalyst}} \equiv Si-O-Si\equiv + H_2$$

In this sense, alkoxide precursors containing Si—H groups show the possibility of using the Si—H groups as an *in situ* reducing agent which allows the formation of metal/silica nanocomposites.[42]

In our study,[40] the *in situ* formation of hydrogen provided by the cleavage of the Si—H bonds was used to generate, during the first step of hydrolysis and condensation reactions, europium in the divalent state.

A typical absorption spectra (Fig. 8) of these is constituted by a broad absorption band in the UV range (200–400 nm) attributed to the $4f^75d^0\rightarrow4f^65d^1$ (Eu^{2+}) transition.

The emission spectra (Fig. 9) of the corresponding hybrids recorded under excitation at 355 nm show a broad emission corresponding to the interconfigurational $4f^65d^1\rightarrow4f^75d^0$ transition centered at 430 nm (*ca.* 23250 cm^{-1}) and a intracon-

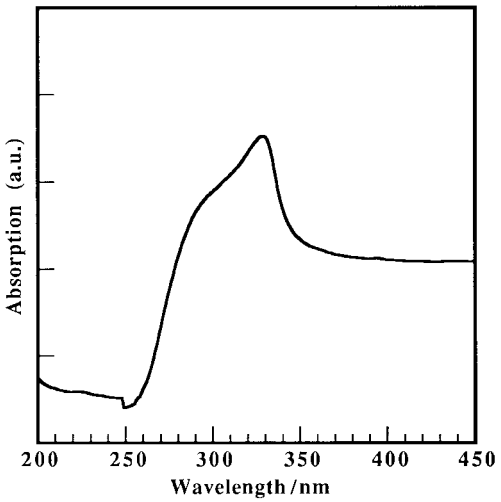

Fig. 8 Absorption spectra of europium doped hybrid xerogels.

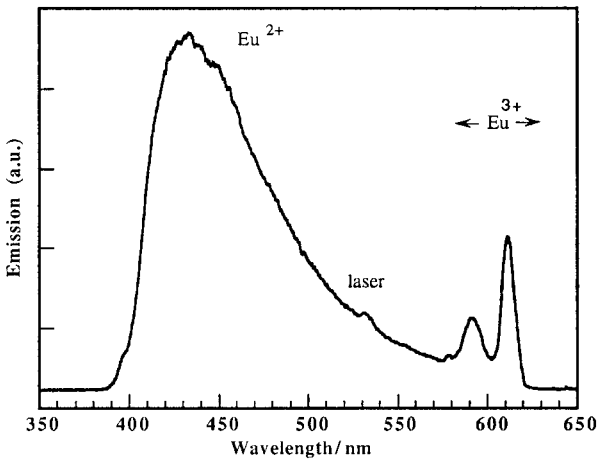

Fig. 9 Emission spectrum of europium doped hybrid xerogel (λ_{exc} = 355 nm).

figurational 4f–4f Eu^{3+} emission in the longer wavelengths. Several bands are obtained corresponding to the $^5D_0 \rightarrow {}^7F_{0,1,2,3}$ transitions. A Stokes' shift value of the Eu^{2+} luminescence around 9000 cm^{-1} is obtained, this shift between the absorption and emission energies of Eu^{2+} located in an oxygen ligand field has been assigned to a combination of crystal field and nephelauxetic effects.[36] These hybrid structures contain oxygen atoms in higher coordination number environments (highly coordinated by metal atoms μ_3-O–Zr/Eu or μ_4-O–Zr/Eu) which produce Eu^{2+} emission at longer wavelengths. Moreover distortion of the oxygen polyhedra from ideal coordination geometry results in a large Stokes' shift. First measurements indicate a $Eu^{2+}:Eu^{3+}$ concentration ratio of about 5:1. The high Eu^{2+} content is probably related to the more efficient reductive medium provided by the initial mixture of the europium trichloride with the MDES and TREOS precursors. Moreover, the intensity of the Eu^{2+} luminescence did not change when the xerogels were stored in air for several months, showing that Eu^{2+} ions are efficiently trapped inside the hybrid matrix.

2-C Quadratic NLO properties of siloxane based hybrids

Most of the sol–gel optics research devoted to non-linear optic (NLO) materials was initially related to third order processes which are compatible with the isotropy of amorphous sol–gel matrices. Organic molecules inside amorphous sol–gel matrices are in general randomly oriented thus ruling out the emission of second harmonic generation. As second order non-linearities are only achieved in a non-centrosymmetric environment, we first demonstrated that orientation of organic chromophores can be performed in hybrid sol–gel matrices[43–46] by using electrical field induced second harmonic (EFISH) or corona electrical field poling techniques. Organic molecules such as *N*-(3-triethoxysilylpropyl)-2,4-dinitrophenylamine (TSDP) were chemically bonded to the oxide backbone of gels. The chemical bonding of the dye to the sol–gel matrix allowed dye concentration to be increased without any crystallization effects.[43–46]

A first generation of sol–gel matrices was synthesized by copolymerization of silicon alkoxysilanes [TSDP and $SiHCH_3(OEt)_2$] and zirconium propoxide precursors.[45] The sols were deposited as transparent coatings and exhibited after corona poling an SHG response of 1.6 pm V^{-1}.[45] Even if in this first generation of sol–gel matrices relaxation of the organic chromophores occurred over several hours, these results suggested the feasibility of poling techniques into hybrid inorganic sol–gel matrices more ionic than classical polymers. Consequently a range of opportunities for the synthesis of optical sol–gel devices with efficient second harmonic properties was discovered. Since then, there has been increasing interest in second order NLO materials synthesized *via* sol–gel chemistry.[47–60]

The optimization of the second order NLO response of hybrid sol–gel matrices with grafted chromophores is currently under investigation by several research groups.

Several strategies are used to improve the NLO response of the hybrid coatings.[43–60] (i) The intrinsic NLO response of the dye can be increase by using chromophores such as *N*-(4-nitrophenyl)-L-prolinol (NPP) or disperse red one (DR1) derivatives which exhibit higher non linearities than nitroaniline ones. (ii) The chromophore relaxation can be controlled by increasing the matrix rigidity. This point is without doubt the most important in order to be able to make efficient NLO devices. The modification of the binary composition (siloxane–crosslinker), the nature of the $M(OR)_4$ crosslinking alkoxide [$SiR'_x(OR)_{4-x}$–$M(OR)_4$: R′=any NLO chromophore; M=Zr, Si, Ti, *etc.*), and the processing of these hybrid materials in the presence of polymers with well known mechanical properties such as methyl methacrylates or polyimides, are the most commonly used strategies to minimize dye relaxation. The strategies we have used to improve the NLO response of hybrid materials will be llustrated in the two following sections.

TSPD/TMOS based hybrids with NLO properties.[58,59] The second generation of hybrids investigated were made *via* hydrolysis and co-condensation of tetramethoxysilane (TMOS) and *N*-(3-triethoxysilylpropyl)-2,4-dinitrophenylamine (TSDP) [Fig. 10(a)] precursors (T and Q are common notations referring to the oxo trifunctional $R'-SiO_3$ and tetrafunctional SiO_4 central units, respectively). FTIR, ^{17}O and ^{29}Si NMR experiments indicated the existence of linear and cyclic siloxane $(T–T)_a$ oligomers and silica $(Q–Q)_b$ units

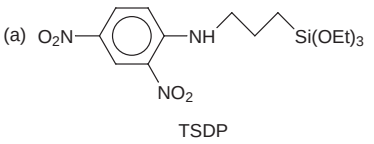

TSDP

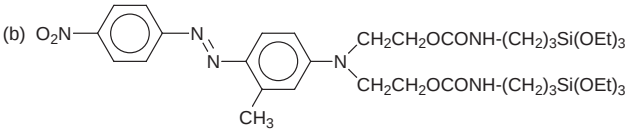

Fig. 10 Graftable NLO dyes: (a)=TSDP (b)=ICTES-Red17.

linked through stable T–O–Q bridges formed in the early stages of the process. Films of thickness 1–5 μm were easily obtained through spin-coating. In such systems gelation probably occurs through the crosslinking of siloxane polymers with Q silica based species. The degrees of condensation of T and Q units measured in the solid state by ^{29}Si MAS NMR spectroscopy are much higher in xerogels than in sols and this difference demonstrates that a large number of condensation and crosslinking reactions still occur upon solvent removal.

The mobility of the NLO chromophores, as observed by high-resolution solid-state ^{13}C NMR spectroscopy, is also correlated with the glass-transition phenomenon of the matrix observed by DSC.[57] This glass transition phenomenon corresponds to the glass transition of the polysiloxane network. T_g, the glass-transition temperature, increases with the TMOS content, while the apparent variation of heat capacity corresponding to T_g decreases. These results, as well as the analysis of the polarization transfer in MAS/CP/DD ^{29}Si NMR experiments, are consistent with the relatively high degree of interpenetration of T and Q units. Therefore, these hybrid TSDP/TMOS coatings can be described as nanocomposites made of silica rich domains and siloxane rich domains. Many Q and T species are mutually sequestered at the nanometer scale. Their microstructure is schematically pictured in Fig. 11. The white parts correspond to the silica-rich phase inside which some T units (black dots) are sequestered. The black spheres correspond to the polysiloxane rich phase which participates in the glass-transition phenomenon and contains Q units (white dots). The sizes of the polysiloxane and silica domains depend not only on the chemical composition but also on the drying procedure and consequently on the solvent and sample thickness.

The TSDP/TMOS ratio, proton concentration, hydrolysis ratio, sequence of mixing the reagents and ageing time of the sol are the chemical parameters that should directly influence a and b values characterizing the lengh of the constituent linear and cyclic siloxane $(T–T)_a$ oligomers and silica $(Q–Q)_b$ units respectively.

However, it has been demonstrated that the mechanical properties of hybrid siloxane–oxide materials, and thus the relaxation behavior of chromophores grafted in these matrices, also strongly depend on their thermal history. Chemical crosslinking is not complete at gelation or even after RT air drying as shown by ^{29}Si NMR experiments.[59] Upon ageing and curing the chemical reactions continue towards completion. Consequently, given sufficient time and temperature to allow mobility of the species a network forming system continues to crosslink long after gelation. The increase of the density of crosslinks modifies the thermomechanical properties of the hybrid as illustrated by the changes observed in T_g upon thermal curing.[57]

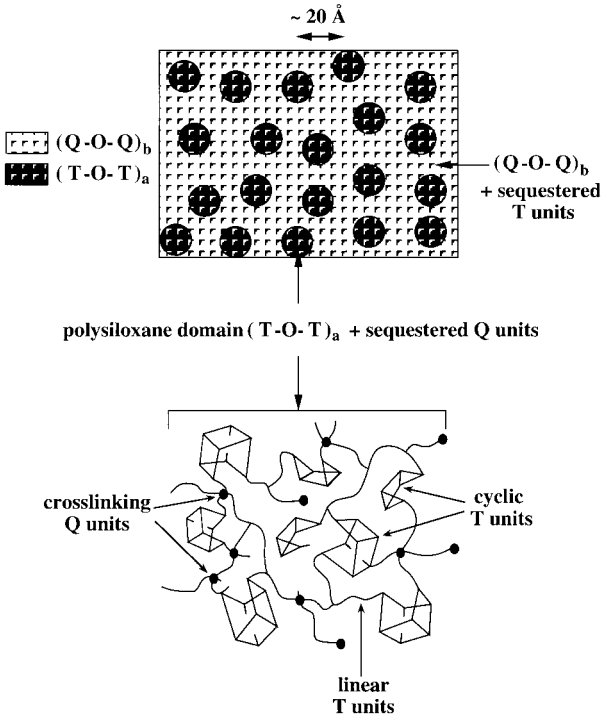

Fig. 11 Schematic representation of TSDP-TMOS based hybrids.[52]

Another processing parameter which has great importance is the electrical field used to poled the NLO chromophores. Accelerated field induced curing must occur in these hybrid TSDP/TMOS materials. The high electrical field provided during poling must favor crosslinking and interpenetration of both polymeric T and Q networks. This was described by Haruvy and co-workers,[48b] who have shown that greatly accelerated curing occurs under ambient conditions on thin films processed from siloxane resins prepared by the sol–gel process when they are exposed to an intense corona-discharge field. The corona cured sol–gel films exhibited a more compact matrix as manifested by the lower mobility of the embedded chromophores and a more hydrophilic surface than thermally cured ones. They suggest that the field induced removal of condensate small molecules and solvents allows better completion of the reactions and more efficient crosslinking.[48]

Compared to the tremendous amount of work and time devoted to polymeric NLO materials, NLO materials made by sol–gel are still in their infancy. For these system, depending on chemical composition, the SHG values range between 2.5 and 10 pm V^{-1}.[47,57] Moreover, the sol–gel materials described in this work have T_g values in the range of 30–70 °C, well below the state of the art obtained with pure organic polymeric materials based on polyimides[61] which are highly non linear and stable for hundred of hours at temperatures higher than 100 °C. However, the excellent knowledge of such systems allowed us within a short period of time to design a third generation of hybrids with a highly improved NLO response.

ICTES-Red17/TMOS based hybrids with NLO properties. The third generation of hybrid organic–inorganic nanocomposites was designed on the basis of the following specifications: the NLO dye must have a high NLO response, it must be anchored by more than one trifunctional link and silica was kept as the crosslinking agent because coatings of better optical quality were usually obtained with binary silica–siloxane materials.[56] In order to be able to perform double grafting of an NLO chromophore, the Red 17 [4-(amino-*N,N*-diethanol)-2-methyl-4′-nitroazobenzene] with a very efficient quadratic hyperpolarizability [$\beta(0)$ (Red 17) = 55×10^{-30} esu] was functionalized with two alkoxysilyl groups by a coupling reaction between the dye and 3-isocyanatopropyltriethoxysilane (ICTES).[56,58] The resulting alkoxysilyl functionalized NLO precursor, ICTES-Red 17 [Fig. 10(b)] was hydrolyzed and co-condensed with TMOS in order to obtain the hybrid siloxane–silica nanocomposite. From the resulting sols, coatings with a thickness of a few μm can be deposited. The resulting hybrid materials do not exhibit T_g according to DSC results.

Non-resonant second-order non-linearities as high as 150–200 pm V^{-1},[58,62] measured on these hybrid systems, with significant long-term stability (10% of signal lost after 20 days) have been reported.[58] The thermal stability at 80 °C has been shown to be excellent, making the ICTES-Red 17/TMOS systems competitive candidates for non-linear optics systems.

Chemical characterization (FTIR, ^{29}Si MAS NMR, UV–VIS spectroscopy) and thermal assisted *in situ* poling studies performed on these coatings revealed the importance of the processing and history of these systems. Three parameters are of paramount importance. (i) Aging of the solution

has been shown to greatly influence the amplitude of the final non-linear signal. This results from improvement of crosslinking efficiency and from modifications of the distribution between cyclic and linear siloxane species. (ii) Thermal precuring of the samples at 150 °C was found to markedly improve the non-linear response as well as its stability. (iii) Optical poling recently tested in sol–gel derived matrices can also be used to improve the chromophore anisotropy[63]

These very reproducible results[58,62] are very promising, however as far as NLO devices are concerned they must be completed by measurements of electro-optical efficiency, waveguiding properties and the evaluation of the optical losses.

3 Tin oxo species based hybrid materials

Tin is a very interesting element because its characteristics make it intermediate between silicon and the transition metals. Like the latter, tin exhibits several coordination numbers (generally from 4 to 6) and coordination expansion makes hydrolysis–condensation reactions of tin alkoxides fast. But, as for silicon, the $Sn–C_{sp^3}$ bond is stable, especially towards nucleophilic agents such as water. This last characteristic allows one to chemically link organic moieties to the tin oxo polymers/oligomers but it also reduces the inorganic functionality of tin and therefore favors the formation of oxo clusters. These oxo clusters can be used as nanobuilding blocks in the design of new hybrid materials.[64–72]

The nanobuilding block $[(RSn)_{12}(\mu_3\text{-}O)_{14}(\mu\text{-}OH)_6]^{2+}$, the structure of which is shown in Fig. 12 can be obtained through several chemical pathways: hydrolysis of $RSn(OPr^i)_3$ or $RSnCl_3$ or by refluxing in toluene butyltin hydroxide oxide [BuSnO(OH)] in the presence of sulfonic acids ($R'SO_3H$)[64–71] and more recently Jousseamme *et al.* opened a new route to this cluster through hydrolysis of functionalized trialkynylorganotin precursors.[72]

This compound is made of a tin oxo-hydroxo cluster with a equal numbers of six- and five-coordinate tin atoms. This cage-like cluster is surrounded by twelve organic chains (butyl, butenyl, *etc.*) which prevent further condensation. Depending on the synthesis conditions the 2+ positive charge can be compensated by a large variety of anions (OH^+,Cl^-, sulfonates, carboxylates, *etc.*). The position of the charge compensating anions in the structure indicates that the 2+ charge is equally located at both cage poles, where six-coordinate tin atoms form hydroxylated $[RSn(OH)]_3O$ trimers.

This cluster is confirmed both in solution by ^{119}Sn NMR [it is characterized by two chemical shifts located at about −280 and −450 ppm (R = butyl or butenyl)] and a set of scalar tin–tin coupling satellites and in the solid state through ^{119}MAS NMR spectroscopy.[69,71] Thus, this cluster can be followed easily throughout the polymerization or crosslinking reactions needed to tranform it into a hybrid material. As a consequence $\{(RSn)_{12}O_{14}(OH)_6\}^{2+}$ is a good nanobuilding block for the synthesis of well defined tin-oxo based hybrid materials that can be used as models.

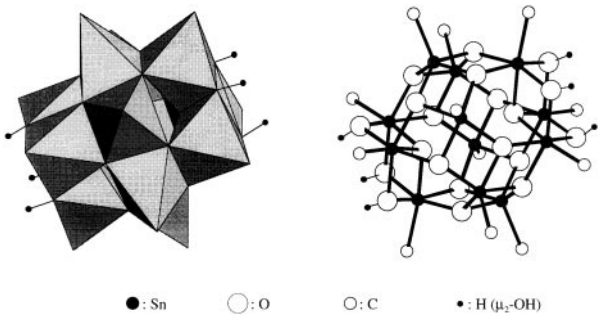

Fig. 12 Molecular structure of $[(RSn)_{12}(\mu_3\text{-}O)_{14}(\mu\text{-}OH)_6]^{2+}$.

Moreover, these clusters exhibit a high versality for the design of hybrids (Fig. 13). $\{(RSn)_{12}O_{14}(OH)_6\}^{2+}2X^-$ can be assembled through organic networks by using the covalent interface provided by the Sn–C bond or by using the ionic interface associated with the charge compensating anions X^- or even by using both interfaces. In the first case the organic moiety carried through the $Sn–C_{sp^3}$ links should be polymerizable (R = butenyl, propylmethacrylate, propylcrotonate, 4-styrylbutyl, *etc.*). In the second case charge compensating organic dianions must be able to bridge the clusters. This can be performed by using dicarboxylates,[65] or α,ω-telechelic macromonomers terminated by carboxylic or sulfonic groups.[67] As an example, the coupling of these clusters by carboxymethyl terminated PEG macromonomers[67] is schematically shown in Fig. 14.

Another strategy could be to use polymerizable anions (methacrylate, 2-acrylamido-2-methylpropane-1-sulfonate, *etc.*) as monomers for organic polymerizations reactions.[66,68a] By a simple acid-base reaction, the oxo-hydroxo butyltin macrocation, $\{(BuSn)_{12}O_{14}(OH)_6\}^{2+}$, was functionalized with 2-acrylamido-2-methylpropane-1-sulfonate, affording nanobuilding blocks with two highly polymerizable groups.[68a]

For the first time,[68a] the direct polymerization of such functionalized oxo-hydroxo butyltin nanoclusters has been successfully performed, yielding hybrid materials in which the nanosized inorganic component is perfectly defined. Two types of organic components are found in such materials. The butyl groups covalently bound onto tin atoms, and, more importantly, poly(2-acrylamido-2-methylpropane-1-sulfonate) chains which interact through electrostatic interactions with the oxo-hydroxo butyltin macrocations and afford the crosslinking.

Such an approach to the construction of tin-based hybrid materials from bifunctional nanobuilding blocks was previously attempted with pure $\{(BuSn)_{12}O_{14}(OH)_6\}$-$\{O_2CC(CH_3)=CH_2\}_2$ but failed as its homopolymerization appeared impossible.[66] Addition of a co-monomer $[CH_3O_2CC(CH_3)=CH_2]$ allowed the polymerization, but recent results have indicated that little crosslinking was achieved, the methacrylate charge compensating anions acting mainly as termination agents.[66b] These difficulties may be related to the fairly large molecular weight of the precursor (*ca.* 2600 g mol^{-1}), but also to the shortness of the methacrylate functional anions which induce high steric hindrance. The second reason seems to prevail, as the use of AAMPS, where the polymerizable acrylamido group is more distant from the anionic anchoring head, allows the formation of a hybrid polymer by simple homopolymerization. More work is currently under way to obtain some information on the average length of the poly(2-acrylamido-2-methylpropane-1-sulfonate) chains, which are probably short owing to strong steric hindrance.

4 Molecular design of transition metal alkoxides for the synthesis of hybrid organic–inorganic copolymers

The chemical tailoring performed with systems containing a Si−C bond cannot be directly extended to pure transition metals because the more ionic M−C bond is broken down upon hydrolysis. Organic modification can however be performed by means of strong complexing ligands. The best are β-diketones and allied derivatives, polyhydroxylated ligands such as polyols, and α- or β-hydroxyacids. These ligands (HL) react readily with transition metal alkoxides $M(OR)_4$ (M = Ce, Ti, Zr, *etc.*) to yield new precursors $M(OR)_{3-x}(L)_x$.[73,74] Upon hydrolysing these new precursors, most of the alkoxy groups are quickly removed while all strong complexing ligands cannot be completely removed. Complexing ligands appear to

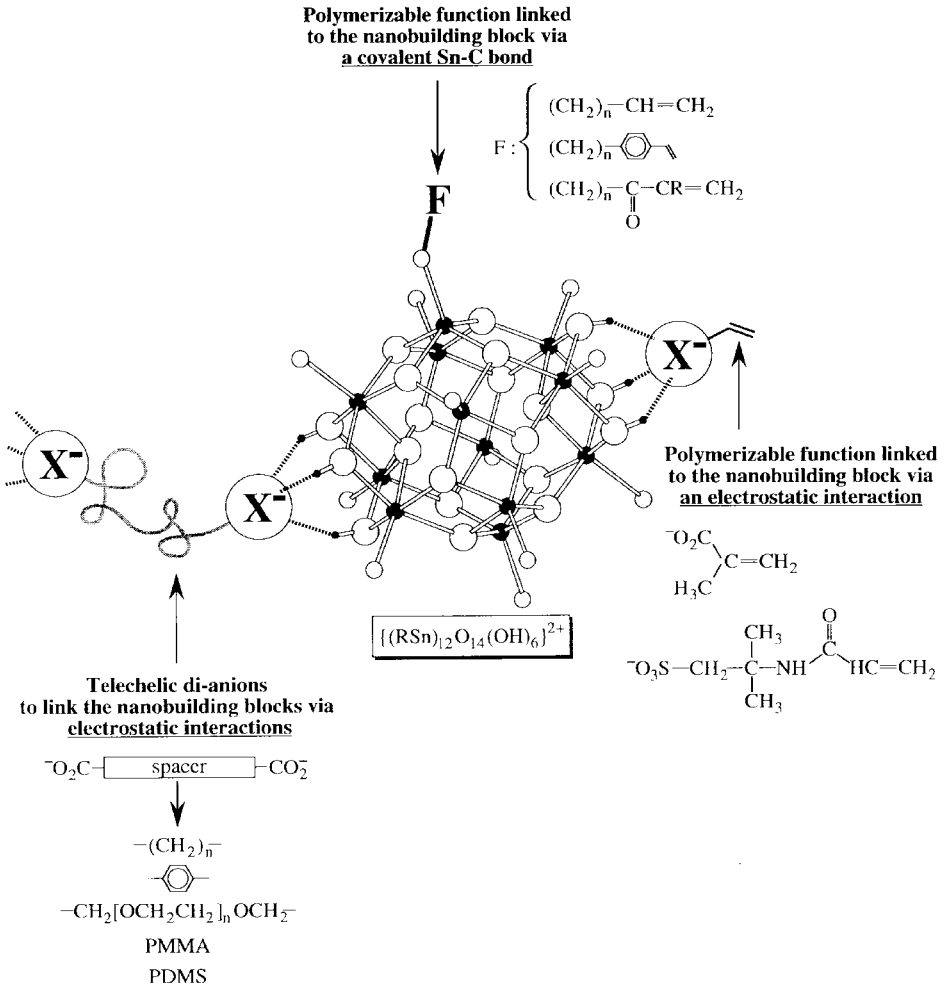

Fig. 13 Schematic representation of the strategies that can be used from a hybrid $[(RSn)_{12}(\mu_3\text{-}O)_{14}(\mu\text{-}OH)_6]^{2+}2X^-$ nanobuilding block.

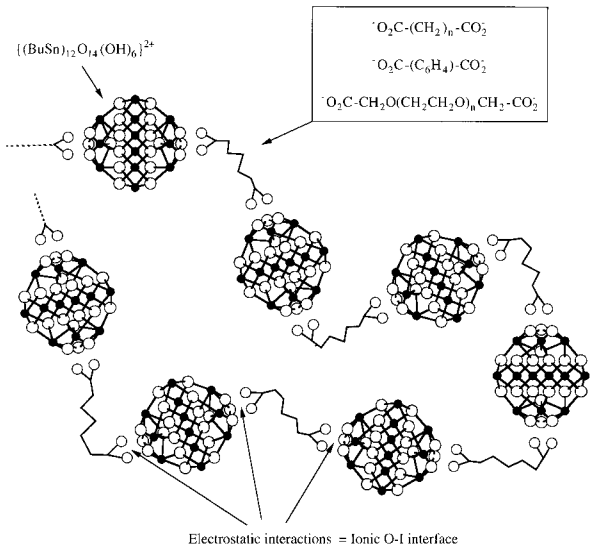

Fig. 14 Schematical representation of the tin oxo-hydroxo clusters hybrids obtained through crosslinking of $[(RSn)_{12}O_{14}(OH)_6]^{2+}$ with α,ω-PEG carboxylates.[67]

be quite stable towards hydrolysis because of chelate and steric hindrance effects. Thus, they allow organic groups to be anchored to transition metal oxo-polymeric species and allow the synthesis of new hybrid organic–inorganic materials.

Organically modified TiO_2 gels, which give photochromic coatings, were synthesized from an allyl acetylacetone modified $Ti(OBu^n)_4$ alkoxide.[74] Double polymerization was performed by partial hydrolysis of the alkoxy groups and radical polymerization of the allyl functions. However polymerization of allyl functions is slow and the degree of polymerization remains low.

More reactive methacrylic acid can also be used as a polymerizable chelating ligand. The sol–gel synthesis of zirconium oxide based monoliths synthesized by UV copolymerization of zirconium oxide sols and organic monomers was recently reported.[8] However, as carboxylic functions are weak ligands, they are largely removed upon hydrolysis[2,75] and thus a large number of the chemical bonds between organic and inorganic networks is lost in the sol state.

Therefore a new approach was chosen with different ligands, such as acetoacetoxyethylmethacrylate (AAEM) and methacrylamidosalicylic acid (MASA), which contain both a strong chelating part and a highly reactive methacrylate group.[6] Zirconium–oxo-PAAEM copolymers were synthesized from zirconium propoxide modified at the molecular level with AAEM.[6] These hybrid organic–inorganic copolymers are made of zirconium oxo-polymers and polymethacrylate chains. The zirconium oxo species, in which zirconium is coordinated to seven oxygens, are chemically bonded to methacrylate chains through the β-diketo complexing function. The complexation ratio (AAEM/Zr) is the key parameter which controls the structure and the texture of these hybrid materials (schematic structure Fig. 15). Careful adjustment of this parameter leads to the tailoring of the ratio between organic and inorganic components and also to zirconium oxo species with more or less open structures. The inorganic/organic ratio increases when the complexation ratio decreases. For a high complexation ratio (0.75) both networks interpenetrate intimately at the nanometer scale, while for a low ratio (0.25) the size of

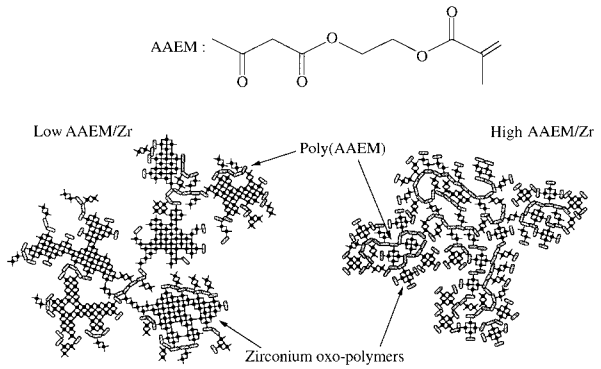

Fig. 15 Schematic structures of class II hybrid materials made from zirconium *n*-propoxide complexed by acetoacetoxyethylmethacrylate (AAEM).[6]

the inorganic domains increases to the sub-micrometer range. Organic and inorganic growths are not independent and such systems probably exhibit similar behavior to the so-called interpenetrating polymer networks.

5 Conclusions

The combination at the nanosize level of inorganic and organic or even bio-active components in a single material makes accessible an immense new area of materials science that has extraordinary implications for developing novel multi-functional materials exhibiting a wide range of properties. This fascinating new field of research brings together scientists working in many different domains. Among soft chemistry processes, sol–gel chemistry offers versatile access to the chemical design of new hybrid organic–inorganic materials. Many new combinations between inorganic and organic or biological components will probably appear in the future. Yet, better understanding and control of the local and semi-local structure of these materials is an important issue, especially if tailored properties are sought.

To achieve such a control of the material structure, the assembly of well defined nanobuilding blocks is an interesting approach. The inorganic components are nanometric and monodispersed. Their structures are perfectly defined, which probably facilitates the characterization of the final materials. The variety found in the nanobuilding blocks (nature, structure, functionality) and links, associated with different assembling strategies, allow very different types of architectures and organic–inorganic interfaces to be formed.[4m] Moreover, the step-by-step preparations of the materials usually allows some control over their semi-local structure. One can also combine the nanobuilding blocks approach with the use of organic templates that self-assemble and allow, through weak forces, control of the assembly step. With the aim of organizing/structuring the nanobuilding blocks prior to their assembly, one can also functionalize them with mesogenic groups and give them self-organizing properties.

As described by Mann *et al*,[76] the traditional view of inorganic solids as condensed matter is currently being reshaped by new insight in materials synthesis.[77–79] A new paradigm, organized matter chemistry, is being formulated. In this field the sol–gel chemistry of organized matter is a very promising field of research which is just beginning to be explored. Hybrids of both Class I and II[4h] and more particularly those obtained through the 'nanobuilding block approach' will have paramount importance in the exploration the theme of 'synthesis with construction' of hierarchically organized (structure and function) materials.

References

1 C. J. Brinker and G. W. Scherrer, *Sol–Gel Science*, *The Physics and Chemistry of Sol–Gel Processing*, Academic Press, San Diego, CA, 1990.

2 (*a*) J. Livage, M. Henry and C. Sanchez, *Prog. Solid State Chem.*, 1988, **18**, 259; (*b*) C. Sanchez, F. Ribot and S. Doeuff, *Inorganic and Organometallic Polymers with Special Properties*, ed. R. M. Laine, NATO ASI Series 206, Kluwer, New York, NY, 1992, p. 267.

3 (*a*) G. L. Wilkes, B. Orler and H. H. Huang, *Polym. Prep.*, 1985, **26**, 300; (*b*) G-S. Sur and J. E. Mark, *Eur. Polym. J.*, 1985, **21**, 1051; (*c*) H. Schmidt, A. Kaiser, H. Patzelt and H. Sholze, *J. Phys.*, 1982, **43**, C9-275.

4 (*a*) B.M. Novak, *Adv. Mater.*, 1993, **5**, 422; (*b*) *Proceeding of the First European Workshop on Hybrid Organic–Inorganic Materials*, ed. C. Sanchez and F. Ribot, *New J. Chem.*, 1994, **18**; (*c*) U. Schubert, N. Hüsing and A. Lorenz, *Chem. Mater.*, 1995, **7**, 2010; (*d*) D. A. Loy and K. J. Shea, *Chem. Rev.*, 1995, **95**, 1431; (*e*) *J. Sol–Gel Sci. Technol.*, 1995, **5**; (*f*) P. Judenstein and C. Sanchez, *J. Mater. Chem.*, 1996, **6**, 511; (*g*) *Matériaux Hybrides*, Série Arago 17, Masson, Paris, 1996; (*h*) C. Sanchez and F. Ribot, *New J. Chem.*, 1994, **18**, 1007; (*i*) U. Schubert, *J. Chem. Soc.*, *Dalton Trans.*, 1996, 3343; (*j*) A. Morikawa, Y. Iyoku, M. Kakimoto and Y. Imai, *J. Mater. Chem.*, 1992, **2**, 679; (*k*) Y. Chujo and T.Saegusa, *Ad. Polym. Sci.*, 1992, **100**, 11; (*l*) *Hybrid Organic–Inorganic Composites*, ed. J. E. Mark, C. Y. C. Lee and P. A. Bianconi, American Chemical Society, Washington, DC, 1995; (*m*) F. Ribot and C. Sanchez, *Comments Inorg. Chem.*, 1998, in press.

5 (*a*) *Better Ceramics Through Chemistry VI*, ed. A. Cheetham, C. J Brinker, M. MacCartney, C. Sanchez, D. W. Schaefer and G. L. Wilkes, *Mater. Res. Soc. Symp. Proc.*, Materials Research Society, Pittsburgh, PA, 1994, vol. 435; (*b*) *Better Ceramics Through Chemistry VII: Organic/Inorganic Hybrid Materials*, ed. B. K. Coltrain, C. Sanchez, D. W. Schaefer and G. L. Wilkes, *Mater. Res. Soc. Symp. Proc.*, Materials Research Society, Pittsburgh, PA, 1996, vol. 435; (*c*) *Sol–Gel Optics I*, ed. J. D. Mackenzie and D. R. Ulrich, Proc. SPIE, Washington, 1990, vol. 1328; (*d*) *Sol–Gel Optics II*, ed. J. D. Mackenzie, Proc. SPIE, Washington, 1992, vol. 1758; (*e*) *Sol–Gel Optics III*, ed. J. D. Mackenzie, Proc. SPIE, Washington, 1994, vol. 2288.

6 (*a*) C. Sanchez and M. In, *J. Non-Cryst. Solids* 1992, **147–148**, 1; (*b*) M. In, C. Gérardin, J. Lambart and C. Sanchez, *J. Sol–Gel Sci. Technol.*, 1995, **5**, 101.

7 (*a*) U. Schubert, E. Arpac, W. Glaubitt, A. Helmerich and C. Chau, *Chem. Mater.*, 1992, **4**, 291; (*b*) C. Barglik-Chory and U. Schubert, *J. Sol–Gel Sci. Technol.*, 1995, **5**, 135.

8 R. Naß and H. Schmidt, in '*Sol–Gel Optics I*', ed. J. D. Mackenzie and D. R. Ulrich, Proc. SPIE, Washington, 1990, vol. 1328, p. 258.

9 H. Schmidt and B. Seiferling, *Mater. Res. Soc. Symp. Proc.*, 1986, **73**, 739.

10 (*a*) D. Levy and D. Avnir, *J. Phys. Chem.*, 1998, **92**, 734; (*b*) D. Levy, S. Einhorn and D. Avni, *J. Non-Cryst. Solids*, 1989, **113**, 137.

11 *Proceedings of the Second International Symposium on Photochromism*, ed. R. C. Bertelson, Chroma Chemicals Inc, Dayton, Ohio, USA, 1997.

12 D. Preston, J. C. Pouxviel, T. Novinson, W. C. Kaska, B. Dunn and J. I. Zink, *J. Phys. Chem.*, 1990, **94**, 4167.

13 H. Nakazumi, R. Nagashiro, S. Matsumoto and K. Isagawa, *Sol–Gel Optics III*, ed. J. D. MacKenzie, Proc. SPIE, Washington, 1994, vol. 2288.

14 L. Hou, B. Hoffmann, M. Menning and H. Schmidt, *J. Sol–Gel Sci. Technol.*, 1994, **2**, 635.

15 L. Hou, B. Hoffmann, H. Schmidt and M. Menning, *J. Sol–Gel Sci. Technol.*, 1997, **8**, 923, 927.

16 L. Hou, M. Menning and H. Schmidt, *Proc Eurogel'92*, 1992, p. 173.

17 J. Biteau, F. Chaput and J. P. Boilot, *J. Phys. Chem.*, 1996, **100**, 9024.

18 D. Levy, *Chem. Mater.*, 1997, **9**, 2666.

19 B. Schaudel, C. Guermeur, C. Sanchez, K. Keitaro and J. Delaire, *J. Mater. Chem.*, 1997, **7**, 61.

20 S. Diré, F. Babonneau, C. Sanchez and J. Livage, *J. Mater. Chem.*, 1992, **2**, 239.

21 F. Babonneau, *Polyhedron*, 1994, **13**, 1123.

22 C. Guermeur and C. Sanchez, forthcoming paper.

23 *Applied photochromic polymers systems*, ed. C. B. McArdle, Gordon and Breach Science Publishers, New York, 1991.

24 S. K. Yuh, E. Bescher, F. Babonneau and J. D. Mackenzie, *Mater. Res. Soc. Symp. Proc.*, 1994, **346**, 803.

25 N. Koslova, B. Viana and C. Sanchez, *J. Mater. Chem.*, 1993, **3**, 111.
26 L. R. Mathews and E. T. Knobbe, *Mater. Res. Soc. Symp. Proc.*, 1993, **286**, 259.
27 I. M. Thomas, S. A. Payne and G. D. Wilke, *J. Non-Cryst. Solids*, 1992, **151**, 183.
28 I. M. Thomas, S. A. Payne and G. D. Wilke, *J. Non-Cryst. Solids*, 1992, **151**, 183.
29 A. A. Kaminskii, in *Laser Crystals*, Springer Verlag, Berlin, Heidelberg, New York, 2nd edn., 1981, pp. 361–433.
30 M. Lecomte, B. Viana and C. Sanchez, *J. Chim. Phys.*, 1991, **88**, 39.
31 B. Viana, N. Koslova, P. Aschehoug and C.Sanchez, *J. Mater. Chem.*, 1995, **5**, 719.
32 C. Guizard, J.C. Achddou, A. Larbot, L. Cot, G. Le Flem, C. Parent and C. L. Lurin, in ref. 5(*c*), p. 208.
33 M. Genet, V. Brandel, M. P. LaHalle and E. Simoni, in ref. 5(*c*), p. 194.
34 W. Nie, B. Dunn, C. Sanchez and P. Griesmar, *Mater. Res. Soc. Symp. Proc.*, 1992, **271**, 639.
35 M. Canva, P. Georges, G. Lesaux, A. Brun, F. Chaput and J. P. Boilot, *J. Non-Cryst. Solids*, 1992, **147**, 627.
36 G. J. Dirksen and G. Blasse, *J. Solid State Chem.*, 1991, **92**, 591.
37 A. Diaz and D. A Keszler, *Chem. Mater.* 1997, **9**, 2071.
38 A. Diaz and D. A Keszler, *Mater. Res. Bull.*, 1996, **31**, 147.
39 H. F. Folkerts and G. Blasse, *J. Mater. Chem.*, 1995, **5**, 1547.
40 E. Cordoncillo, P. Escribano, B. Viana and C. Sanchez, *J. Mater. Chem.*, 1998, **8**, 1507.
41 J. Chrusciel and Z. Lasocki, *Pol. J. Chem.*, 1983, **57**, 121.
42 R. Campostrini and S. Diré, *Eurogel Proceedings, Advanced Materials and Processes by Sol–Gel Techniques*, Colmar, 1992, ed. S. Vilminot, Strasbourg, 1995, p. 307.
43 G. Pucetti, I. Ledoux, J. Zyss, P. Griesmar and C. Sanchez, *Polym. Prepr.*, 1991, **32**, 61.
44 J. Zyss, G. Pucetti, I. Ledoux, P. Griesmar, J. Livage and C. Sanchez, *Fr. Pat.*, 1152, March 1991.
45 (*a*) E. Toussaere, J. Zyss, P. Griesmar and C. Sanchez, *Non Linear Optics*, 1991, **1**, 349; (*b*) C. Sanchez, P. Griesmar, E. Toussaere, G. Puccetti, I. Ledoux and J. Zyss, *Non Linear Optics*, 1992, **4**, 245.
46 P. Griesmar, C. Sanchez, G. Pucetti, I. Ledoux and J. Zyss, *Mol. Eng.*, 1991, **1**, 205.
47 (*a*) J. Kim, J. L. Plawsky, R. LaPeruta and G. M. Korenowski, *Chem. Mater.*, 1992, **4**, 249; (*b*) J. Kim, J. L. Plawsky, E. Van Wagenen and G. M. Korenowski, *Chem. Mater.*, 1993, **5**, 1118.
48 (*a*) Y. Haruvy and S. E. Weber, *Mater. Res. Soc. Symp. Proc.*, 1992, **271**, 297; (*b*) Q. Hibben, E. Lu, Y. Haruvy and S.E. Weber, *Chem. Mater.*, 1994, **6**, 761.
49 F. Chaput, D. Riehl, Y Levy and J. P. Boilot, *Chem. Mater.*, 1993, **5**, 589.
50 Y. Zhang, P. N. Prasad and R. Burzynski, *Chem. Mater.*, 1992, **4**, 851.
51 Y. Nosaka, N. Tohriiwa, T. Kobayashi and N. Fujii, *Chem. Mater.*, 1993, **5**, 930.
52 S. Marturunkakul, J. I. Chen, R. J. Jeng, S. Sengupta, J. Kumar and S. K. Tripathy, *Chem. Mater.*, 1993, **5**, 743; K. Izawa, N. Okamoto and O. Sugihara, *Jpn. J. Appl. Phys.*, 1993, **32**, 807.
53 L. Kador, R. Fischer, D. Haarer, R. Kaseman, S. Brück, H. Schmidt and H. Dürr, *Adv. Mater.*, 1993, **5**, 270.
54 (*a*) J. R. Caldwell, R. W. Cruse, K. J. Drost, V. P. Rao, A. K.-Y. Jen, K. Y. Wong, Y. M. Cali, R. M. Mininni, J. Kenney, E. Binkley, L. R. Dalton, Y. Shi and W. H. Steier, *Mater. Res. Soc. Symp. Proc.*, 1994, **328**, 531; (*b*) Z. Yang, C. Xu, B. Wu, L. R. Dalton, S. Kalluri, W. H. Steier, Y. Shi and J. H. Bechtel, *Chem. Mater.*, 1994, **6**, 1899; (*c*) H. W. Oviatt, K. J. Shea, S. Kalluri, Y. Shi, W. Steier and L. R. Dalton, *Chem. Mater.*, 1995, **7**, 493.
55 (*a*) F. Chaput, D. Reihl, Y. Levy and J.-P. Boilot, *Chem. Mater.*, 1993, **5**, 589; (*b*) D. Reihl, F. Chaput, Y. Levy, J.-P. Boilot, F. Kajzar and P. A. Chollet, *Chem. Phys. Lett.*, 1995, **245**, 36.
56 (*a*) B. Lebeau, C. Sanchez, S. Brasselet, J. Zyss, G. Froc and M. Dumont, *New J. Chem.*, 1996, **20**, 13; (*b*) B. Lebeau, C. Sanchez, S. Brasselet and J. Zyss, *Mater. Res. Soc. Symp. Proc.*, 1996, **435**, 395; (*c*) B. Lebeau, C. Guermeur and C. Sanchez, *Mater. Res. Soc. Symp. Proc.*, 1994, **346**, 315.
57 B. Lebeau, J. Maquet, C. Sanchez, E. Toussaere, R. Hierle and J. Zyss, *J. Mater. Chem.*, 1994, **4**, 1855.
58 B. Lebeau, C. Sanchez, S. Brasselet and J. Zyss, *Chem. Mater.*, 1997, **9**, 1012.
59 B. Lebeau, J. Maquet, C. Sanchez, F. Beaume and F. Lauprêtre, *J. Mater. Chem.*, 1997, **7**, 989.
60 C. Sanchez and B.Lebeau, *Pure Appl. Opt.*, 1996, **5**, 689.
61 R. F. Shi, M. H. Wu, S. Yamada, Y. M. Cai and A. F. Garito, *Appl. Phys. Lett.*, 1993, **63**, 1173.
62 D. Blanc, P. Peyrot, C. Sanchez and C. Gonnet, *Opt. Eng. Integrated Opt.*, 1998, **37**, 1203.
63 C. Fiorini, F. Charra, J. M. Nunzi, I. D. W. Samuel and J. Zyss, *Opt. Lett.*, 1995, **20**, 2469.
64 F. Ribot, F. Banse and C. Sanchez, *Mater. Res. Soc. Symp. Proc.*, 1994, **346**, 121.
65 F. Ribot, F. Banse, F. Diter and C. Sanchez, *New J. Chem.*, 1995, **19**, 1145.
66 (*a*) F. Ribot, F. Banse, C. Sanchez, M. Lahcini and B. Jousseaumme, *J. Sol–Gel Sci. Technol.*, 1997, **8**, 529; (*b*) L. Angiolini, D. Caretti, C. Carlini, R. De Vito, F. T. Niesel, E. Salatelli, F. Ribot and C. Sanchez, *J. Inorg. Organomet. Polym.*, 1998, **7**, 151.
67 (*a*) F. Ribot,C. Eychenne-Baron and C. Sanchez, *Mater. Res. Soc. Symp. Proc.*, 1996, **435**, 43; C. Eychenne-Baron, F. Ribot and C. Sanchez, *J. Organomet. Chem.*, 1998, **567**, 137.
68 F. Ribot, C. Eychenne-Baron and C. Sanchez, *Mater. Res. Soc. Symp. Proc.*, 1998, **519**, in press.
69 F. Banse, F. Ribot, P. Tolédano, J. Maquet and C. Sanchez, *Inorg. Chem.*, 1995, **34**, 6371.
70 H. Puff and H. Reuter, *J. Organomet. Chem.*, 1989, **373**, 173.
71 D. Dakternieks, H. Zhu, E. R. T. Tiekink and R. J. Colton, *J. Organomet. Chem.*, 1994, **476**, 33.
72 P. Jaumier, B. Jousseaume, M. Lahcini, F. Ribot and C. Sanchez, *Chem. Commun.*, 1998, 369.
73 (*a*) R.C. Mehrotra, R. Bohra and D. P. Gaur, *Metal β-diketonates and Allied Derivatives*, Academic Press, London, 1978; (*b*) D. C. Bradley, R. C. Mehrotra and D. P. Gaur, *Metal Alkoxides*, Academic Press, London, 1978; (*c*) L. G. Hubert-Pfalzgraf, *New J. Chem.*, 1987, **11**, 663; (*f*) A. Leaustic, F. Babonneau and J. Livage, *Chem. Mater.*, 1989, **1**, 248; (*g*) F. Ribot, P. Tolédano and C. Sanchez, *Chem. Mater.*, 1991, **3**, 759; (*h*) C.Sanchez, M. In, P. Toledano and P. Griesmar, *Mater. Res. Soc. Symp. Proc.*, 1992, **271**, 669.
74 C. Sanchez, J. Livage, M. Henry and F. Babonneau, *J. Non-Cryst. Solids*, 1988, **100**, 650.
75 S. Doeuff, M. Henry, C. Sanchez and J. Livage, *J. Non-Cryst. Solids*, 1987, **89**, 206.
76 S. Mann, S. L. Burkett, S. A. Davis, C. E. Fowler, N. H. Mendelson, S. D. Sims, D. Walsh and N. T. Whilton, *Chem. Mater.*, 1997, **9**, 2300.
77 S. Mann and G. A. Ozin, *Nature*, 1996, **382**, 313.
78 C. G. Göltner and M. Antonietti, *Adv. Mater.*, 1997, **9**, 431.
79 (*a*) A. Monnier, F. Schuth, Q. Huo, D. Kumar, D. Margolese, R. S. Maxwell, G.D. Stucky, M. Krishnamurty, P. Petroff, A. Firouzi, M. Janicke and B. F. Chmelka, *Science*, 1993, **261**, 1299; (*b*) A. Firouzi, D. Kumar, L. M. Bull, T. Besier, P. Sieger, Q. Hue, S. A. Walker, J. A. Zasadinski, C. Glinka, J. Nicol, D. Margolese, G. D. Stucky and B. F. Chmelka, *Science*, 1995, **267**, 1133; (*c*) D. Y. Zhao, P. D. Yang, Q. S. Huo, B. F. Chmelka and G. D. Stucky, *Curr. Opin. Solid State Mater. Sci.*, 1998, **3**, 111; (*d*) C. J. Brinker, *Curr. Opin. Colloid Interface Sci.*, 1998, **3**, 166; (*e*) Y. Lu, R. Ganguli, C. A. Drewien, M. T. Anderson, C. J. Brinker, W. Gong, Y. Guo, H. Soyez, B. Dunn, M. H. Huang and J. I. Zink, *Nature*, 1997, **389**, 364; (*f*) G. H. Mehl and J. W. Goodby, *Chem. Ber.*, 1996, **129**, 521.

Paper 8/05538F